Brillouin scattering in Co/Cu/Co and Co/Au/Co trilayers: Anisotropy fields and interlayer magnetic exchange

Y. Roussigné, F. Ganot, C. Dugautier, and P. Moch
Laboratoire des Propriétés Mécaniques et Thermodynamiques des Matériaux CNRS, Université Paris-Nord, 93430 Villetaneuse, France

D. Renard
Institut d'Optique Théorique et Appliquée, Université Paris-Sud, 91405 Orsay, France
(Received 30 January 1995)

Magnetic anisotropies and interlayer exchange interaction are derived from Brillouin-scattering spectra of various thin films with one or two Co magnetic layers, evaporated in ultrahigh vacuum. The oscillatory behavior of the interlayer exchange interaction is observed in Co/Au/Co sandwiches; the measured values of the pseudoperiod (9.6 Å) and of the attenuation length (12 Å) agree well with recent determination by magneto-optical and magnetoresistive measurements and with theoretical predictions.

INTRODUCTION

Brillouin-scattering spectroscopy is one of the most powerful methods to derive the parameters which monitor the physical properties of thin films containing magnetic layers. On the one hand, among these parameters the anisotropy and, for multilayered structures, the interlayer magnetic exchange play a major role and a proper choice of these quantities allows one to develop various devices based on magneto-optics and magnetoresistance. The volume and the surface anisotropies show a large variety of behaviors depending upon the crystallographic structures, their orientation, their thickness, and their roughness, and they have given rise to a number of experimental and theoretical publications where the demagnetizing, magnetocrystalline, and magnetoelastic contributions are analyzed.[1–9] On the other hand, the interlayer exchange depends upon the interlayer spacer in a nontrivial way: in many cases an oscillatory variation has been observed.[10–14] It is often interpreted in terms of a Ruderman-Kittel-Kasuya-Yosida (RKKY) mechanism.[15] Up to now, the most studied magnetic layers are probably Fe and Co films and the determination of an oscillatory behavior of the exchange by Brillouin scattering was evidenced on Fe/Cu/Fe and Fe/Cr/Fe sandwiches.[16–18]

The present Brillouin study deals with textured magnetic Co layers evaporated in ultrahigh vacuum: the sublayers and/or the interlayers (in the case of sandwiched composites) consist of Cu or Au films; the cobalt layers show crystallographic characteristics approaching a fcc (or a hcp) structure with a ⟨111⟩ (or a ⟨0001⟩) axis normal to the surface. Concerning these types of Co films, the published experimental data, derived from various techniques, are subject to a large dispersion which is not completely understood. The anisotropy is generally found as uniaxial and easy axis,[1,4,6–9,19,20] but its value and the relative contributions of the surface and of the volume terms are controversial. Particularly, the measured volume anisotropy suffers large variations depending upon the crystallographic structure and upon the magnetoelastic contribution. The oscillatory variation of the interlayer exchange energy in Co/Cu/Co structures was clearly observed through the magneto-optical Kerr effect on sandwiches and through magnetoresistance studies in superlattices; however, pinhole defects can easily prevent its observation.[21] In the case of Co/Au/Co structures, a clearly oscillatory exchange was evidenced only recently.[10]

There are several Brillouin studies of Co layers or multilayers.[2,4,22–25]. They often involve superlattices, which complicates the interpretation of the observed spectra: up to now, the oscillatory variation of the interlayer exchange was measured in Co/Ru multilayers.[13] Finally, accurate Brillouin measurements of the anisotropy of Co layers have been performed[8,9] but generally they only involve ultrathin films.

The study presented in this paper is restricted to samples consisting of one or two magnetic layers and of appropriate nonmagnetic sublayers and/or spacer, in order to allow an optimal determination of the anisotropies and of the exchange interaction. In the next section we present the studied structures and the experimental setup. Section II deals with the calculation of the shapes of the Brillouin spectra. In the last section we present the experimental data and we discuss the results concerning anisotropy and interlayer exchange.

I. SAMPLE PREPARATION AND EXPERIMENTAL SETUP

Co/Cu/Co and Co/Au/Co trilayers have been prepared by ultrahigh vacuum evaporation. The substrates consisted of oxidized Si or float glass plates. In this last case, the roughness, as measured by atomic force microscopy, is lower and the results can be more directly compared with measurements by other methods but unfortunately, due to the low thermal conductivity of glass, the Brillouin study has to be performed using very low illuminating powers (100 mW or less) in order to avoid undesirable heating and, due to this experimental difficulty, only few spectra have been obtained.

The substrates are plated with a 250 Å annealed Au

0163-1829/95/52(1)/350(11)/$06.00

buffer. When Co is directly evaporated on such Au buffers, a quasihexagonal epitaxy of the deposited magnetic layer is obtained.[1,4,19,20] In contrast, with an intermediate thin Cu film (30 Å), the epitaxy approaches the fcc structure. A more detailed analysis includes structural defects, the density of which depends upon the conditions of preparation and increases with the Co thickness. Such behavior was confirmed by NMR measurements[26] and, as discussed below, is indirectly verified through our Brillouin results. Taking advantage of these differences, we have then studied various available combinations of the structures of the magnetic layers. In all cases, the samples were finally top protected by a thin Au layer (30 Å).

Concerning the thicknesses of the magnetic layers and of the nonmagnetic spacer, they were carefully adapted to insure appropriate measurements of the anisotropies and of the interlayer exchange. In order to measure the anisotropy field, samples showing a set of steplike variations of the magnetic layers were prepared (see Fig. 1). The interlayer magnetic exchange was studied using samples showing a set of steplike variations of the interlayer thickness.

The Brillouin magnetic back-scattered polarized spectra were studied using a conventional 5-pass or a (2×3)-passes tandem Fabry-Pérot interferometer. The samples were illuminated by a single-mode Ar^+ laser, using powers ranging from 20 to 500 mW at a wavelength of 5145 Å. Reliable spectra were obtained with recording times varying from 2000 to 10 000 s. A magnetic field **H** up to 0.7 T was applied parallel to the films.

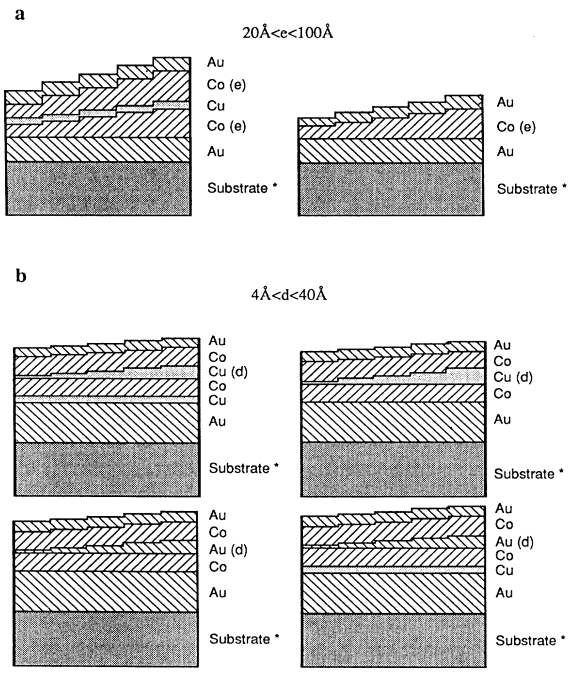

FIG. 1. Typical studied structures. (a) Samples with variable thickness of the magnetic layer(s) (steplike variation with 10 Å steps: $20 < e < 100$ Å) designed in order to study the anisotropy. (b) Samples with variable thickness of the nonmagnetic spacer (steplike variation with 2 Å steps: $4 < d < 40$Å) designed in order to study the interlayer exchange. The substrate is oxidized Si [Si/SiO_2 (2000 Å)] or float glass.

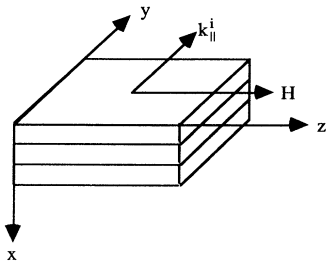

FIG. 2. Geometrical arrangement for the in-plane component of the incident-light wave vector ($k_{\parallel}^{i}$) and the applied magnetic field (H).

The following notations are used in this paper. **H** is applied along the $\mathbf{e}_z$ axis (see Fig. 2) and the in-plane component $\mathbf{k}_{\parallel}^{i}$ of the wave vector $\mathbf{k}^i$ of the incident light is parallel to the $\mathbf{e}_y$ axis. With our geometrical arrangement $\mathbf{k}^s = -\mathbf{k}^i$ where $\mathbf{k}^s$ is the wave vector of the observed scattered light. The observed magnetic excitations then propagate along the films with a wave vector $\pm\mathbf{Q}_{\parallel} = \pm 2\mathbf{k}_{\parallel}^{i}$; its amplitude $Q_{\parallel} = 2k^i \sin\theta$ (where θ is the angle between $\mathbf{k}^i$ and the direction $\mathbf{e}_x$, normal to the sample) can be varied by rotating the sample around the $\mathbf{e}_z$ axis. Most of the spectra were taken using $\theta = 45°$, which leads to $Q_{\parallel} = 1.73 \times 10^5$ cm^{-1}.

II. MODELS FOR FREQUENCY AND INTENSITY CALCULATIONS

A. Frequencies of the magnetic excitations

They are calculated in the usual way from the linearized Landau-Lifshitz equation, taking into account the Maxwell equations in the magnetostatic approximation and the appropriate boundary conditions at the interfaces of the layers.[27,28] One writes

$$\frac{i\omega}{\gamma}\mathbf{m} = \mathcal{M} \times \mathbf{H}_{ef} \tag{1}$$

where ω is the angular frequency and **m** is the oscillating magnetization around its static value **M** ($\mathcal{M} = \mathbf{M} + \mathbf{m}$). γ is an effective gyromagnetic factor. In the studied case the applied static field **H** is high enough to insure that **M** is parallel to the film and that, consequently, the static demagnetizing field vanishes. With these conditions the effective field $\mathbf{H}_{ef}$ is written as

$$\mathbf{H}_{ef} = \mathbf{h}_d - \nabla_{\mathcal{M}} U^{av} + \frac{D}{M}\nabla^2\mathbf{m} + \mathbf{H} , \tag{2}$$

where $\mathbf{h}_d$ is the oscillating demagnetizing field subject to

$$\nabla\cdot(\mathbf{h}_d + 4\pi\mathbf{m}) = 0, \quad \nabla \times \mathbf{h}_d = \mathbf{0} . \tag{3}$$

U^{av} is the volume anisotropy energy density and

$$\frac{D}{2M}\left[\left[\frac{\partial \mathbf{m}}{\partial x}\right]^2+\left[\frac{\partial \mathbf{m}}{\partial y}\right]^2+\left[\frac{\partial \mathbf{m}}{\partial z}\right]^2\right]$$

is the ferromagnetic exchange energy density.

The boundary conditions derive from the Maxwell equations [continuities of the tangential components of $\mathbf{h}_d$ and of the normal component of $(\mathbf{h}_d+4\pi\mathbf{m})$] and from the Rado-Weertman relation[27,28]

$$\mathcal{M}\times\left[-\nabla_{\mathcal{M}}U^{as}+\frac{D}{\mathcal{M}}\frac{\partial \mathcal{M}}{\partial n}\right]=0\ . \tag{4}$$

U^{as} is the surface anisotropy energy density and $\mathbf{n}$ is normal to the film and directed from the nonmagnetic to the magnetic material ($\mathbf{n}=\pm\mathbf{e}_x$).

More specifically, an additional index (1 or 2) has to be used in order to label each magnetic layer and, for surfaces submitted to an interlayer magnetic exchange, Eq. (4) has to be replaced by the Hoffmann relation,[27,28] i.e.,

$$\mathcal{M}_i\times\left[-\nabla_{\mathcal{M}}U_i^{as}+\frac{D}{\mathcal{M}}\frac{\partial \mathcal{M}_i}{\partial n_i}+\frac{2A_{12}}{\mathcal{M}^2}\mathcal{M}_j\right]=0\ ,$$

$$i,j=1,2\ (j\neq i)\ , \tag{5}$$

where $\mathcal{M}_1$ and $\mathcal{M}_2$ are the surface magnetizations of the interacting layers and where $-(2A_{12}/\mathcal{M}^2)\mathcal{M}_1\cdot\mathcal{M}_2$ is the exchange surface energy density.

The solutions of the linearized equations were numerically calculated assuming the following forms for the anisotropy energies:

$$U^{as}=-\frac{k}{\mathcal{M}^2}\mathcal{M}_x^2\ , \tag{6a}$$

$$U^{av}=-\frac{K}{\mathcal{M}^2}\mathcal{M}_x^2\ . \tag{6b}$$

k and K are the surface and the volume anisotropy constants, respectively. Concerning the magnetocrystalline contribution to anisotropy the $\mathcal{M}_x^2$ dependence is certainly appropriate for a hexagonal structure with its $\langle 0001\rangle$ axis along the normal of the film: such a situation is generally observed for a Co layer deposited on a Au film normal to a cubic $\langle 111\rangle$ axis.[1,4,19,20] When Au is replaced by Cu, the Co layer shows a structure approaching the fcc arrangement with a $\langle 111\rangle$ axis normal to the layer: a more accurate description[26] leads to a "mixed" behavior between a purely fcc and a purely hexagonal layer. This leads to the form (6b) for the volume magnetocrystalline contribution rather than to a purely cubic biquadratic form, but with a value of K significantly reduced compared to the Au-Co situation, as confirmed by our experiments. On the other hand, the magnetoelastic lower-order terms can be shown to vary as $\mathcal{M}_x^2$.[20] It is also noteworthy that higher-order uniaxial terms ($\propto\mathcal{M}_x^4$) have been reported to be non-negligible. However, the expected values of anisotropy in the studied structures lead to a static magnetization $\mathbf{M}$ parallel to the applied field $\mathbf{H}$ and it can be proved that, for these studied configurations, the higher-order uniaxial terms do not influence the frequencies of the magnetic excitations; consequently, they have been omitted in (6a) and (6b).

For the studied thicknesses only the two lowest modes lie in the Brillouin frequency range: both are sensitive to the anisotropy values, but only one of them significantly depends upon A_{12} (quasiuniform mode).

As numerically verified on our data, an alternative simplified treatment provides nearly identical results: it consists in suppressing U^{as} in (4) or (5) and in replacing U^{av} by an effective anisotropy energy density $\tilde{U}^{av}$ in each layer, such as

$$\tilde{U}^{av}=U^{av}+\frac{1}{e}[U^{as+}+U^{as-}]=U^{av}+\frac{2}{e}U^{as}\ , \tag{7}$$

where U^{as+} and U^{as-} are the surface anisotropy energies on each side of the layer of thickness e. The uncertainties arising from our experimental data do not allow us to make a distinction between the two models. Indeed, in the last term of expression (7) the localization of the energy terms varying as $1/e$ is completely lost. Such an approach may be more realistic since the localization of the strain-induced magnetoelastic terms, which significantly contribute to this dependence when using rather thick films, is not clearly specified.[19,20] Consequently, we write

$$\tilde{U}^{av}=-\frac{\tilde{K}(e)}{\mathcal{M}^2}\mathcal{M}_x^2\ , \tag{8a}$$

where in large intervals of thicknesses, $\tilde{K}(e)$ often takes the form

$$\tilde{K}(e)=K+\frac{2k}{e}\ . \tag{8b}$$

But, as discussed in the next section, it is generally not possible to assume that $2k=k^++k^-$, where k^+ and k^- refer to two different interfaces: such a partition between k^+ and k^- is probably correct only for very thin samples where the magnetoelastic contribution to k vanishes and where the "surface" term k has a Néel-type magnetocrystalline origin. The numerical results are calculated versus $\tilde{K}$ and A_{12}, assuming that γ, M, and D keep the values found in bulk Co ($\gamma=1.90\times10^7$ Hz G^{-1}, $4\pi M=17\,600$ G, $D=2.6\times10^{-9}$ G cm^2).[29] It is also convenient to introduce an effective anisotropy field

$$\tilde{H}_a(e)=2\tilde{K}(e)/M\ . \tag{9}$$

As pointed out at the end of the preceding section the calculated frequencies correspond to excitations propagating along the surface with a wave vector $\mathbf{Q}_\parallel$. For identical layers ($\tilde{H}_{a1}=\tilde{H}_{a2}$) the frequencies do not change when changing $\mathbf{Q}_\parallel$ into $-\mathbf{Q}_\parallel$. As a result, the observed Stokes and anti-Stokes lines have the same frequency (it can be easily seen that the positive solutions for ω refer to Stokes or anti-Stokes spectra for $\mathbf{Q}_\parallel$ or $-\mathbf{Q}_\parallel$, respectively; alternatively, Stokes and anti-Stokes frequencies are, respectively, the positive and the negative solutions for the frequencies at a given $\mathbf{Q}_\parallel$). In contrast, with nonidentical layers ($\tilde{H}_{a1}\neq\tilde{H}_{a2}$) one finds different values for the Stokes and the anti-Stokes frequencies. This difference will be exploited in the next section in order to calculate separately $\tilde{H}_{a1}$ and $\tilde{H}_{a2}$ and we shall show that $\tilde{H}_a$ significantly depends upon the substrate (Cu or Au) on which the layer has been evaporated.

B. Shapes and intensities of the spectra

As experimentally verified, the shapes and the intensities of the spectra strongly depend upon the magnetic, optic, and geometrical parameters characterizing the studied layered structure. In order to predict and to analyze the spectra, it is necessary to proceed to a rather complete calculation which, indeed, involves the evaluation of the Fourier transforms of the correlation functions of various magnetization components.

The modulation of the electric polarization (or, equivalently, of the permittivity) by the exciting electric field $\mathbf{E}^i$ is written as

$$4\pi P_\alpha = A_{\alpha\beta\gamma}\mathcal{M}_\gamma E^i_\beta \ , \tag{10}$$

where the symmetry properties of $A_{\alpha\beta\gamma}$ depend upon the crystal structure. In the isotropic and in the cubic cases $A_{\alpha\beta\gamma}=A\epsilon_{\alpha\beta\gamma}$, where A is a (light-frequency-dependent) constant and where $\epsilon_{\alpha\beta\gamma}$ is the totally antisymmetric (Levi-Civita) tensor. Such a form leads to well-known selection rules for the scattered light: with the experimental arrangement used, the scattered light is polarized perpendicularly to the incident beam. For a hexagonal uniaxial structure the form of the $A_{\alpha\beta\gamma}$ tensor is less simple and depends upon two distinct constants: as a result, the selection rules for the scattered light are modified. From our experimental data it appears that a discrepancy from cubic selection rules does exist with some studied samples but, in all cases, it remains very small: consequently, in the following we shall use the cubic approximation which will be shown to provide a good agreement with the experiments. The Fourier transform of the electric scattered field can be written[30]

$$\mathbf{E}^s(x,\mathbf{k}^s_\parallel,\omega^s)=4\pi\left[\frac{\omega^i}{c}\right]^2 \times\int d^3\mathbf{r}'dt'\overline{\overline{D}}(x,x',\mathbf{k}^s_\parallel,\omega^s)\mathbf{P}(\mathbf{r}',t') \times\exp(-i\mathbf{k}^s_\parallel\cdot\mathbf{r}'_\parallel+i\omega^s t') \ , \tag{11}$$

where the components $D_{\alpha\beta}$ of $\overline{\overline{D}}$ are the Green functions associated with the operator

$$\left[\frac{\omega^s}{c}\right]^2\varepsilon(x)-\nabla\times\nabla\times \quad \text{with } \nabla=\left[\frac{\partial}{\partial x}\right]\mathbf{e}_x+i\mathbf{k}^s_\parallel \tag{12}$$

[$\varepsilon(x)$ is the permittivity].

If the exciting field in the magnetic material is

$$\mathbf{E}^i(\mathbf{r})=\mathbf{E}^i(x)\exp(i\mathbf{k}^i_\parallel\cdot\mathbf{r}_\parallel-i\omega^i t)$$

the scattered intensity at the frequency ω^s is found to be proportional to

$$\sum_{\alpha\beta\gamma\delta\varepsilon\zeta\eta} A\,A^*\epsilon_{\beta\delta\varepsilon}\epsilon_{\gamma\zeta\eta}\int dx'dx''D_{\alpha\beta}(x,x')D^*_{\alpha\gamma}(x,x'') \times E^i_\delta(x')E^{*i}_\zeta(x'')\langle m^*_\eta m_\varepsilon\rangle_{\omega\mathbf{Q}_\parallel} \ , \tag{13}$$

where

$$\langle m^*_\eta m_\varepsilon\rangle_{\omega\mathbf{Q}_\parallel}=\int dt''d^2\mathbf{r}''_\parallel\langle m^*_\eta(x'',\mathbf{r}''_\parallel,t'') \times m_\varepsilon(x',\mathbf{r}'_\parallel=\mathbf{0},t'=0)\rangle \times\exp[i(-\mathbf{Q}_\parallel\mathbf{r}''_\parallel+\omega t'')] \tag{14}$$

with $\omega=\omega^i-\omega^s$. The fluctuation-dissipation theorem provides (for $\hbar\omega\ll k_BT$, which is the case in Brillouin-scattering experiments)

$$\langle m^*_\eta m_\varepsilon\rangle_{\omega\mathbf{Q}_\parallel}\propto\frac{k_BT}{\omega}\mathrm{Im}\chi_{\eta\varepsilon}(x'',x',\mathbf{Q}_\parallel,\omega) \ . \tag{15}$$

$\chi_{\eta\varepsilon}$ is an appropriate susceptibility;

$$m_\eta(x'',\mathbf{Q}_\parallel,\omega)=\chi_{\eta\varepsilon}(x'',x',\mathbf{Q}_\parallel,\omega)h_{p\varepsilon}(x',\mathbf{Q}_\parallel,\omega) \ ,$$

where $\mathbf{h}_p\delta(x''-x')$ is a spatial Fourier transform of a probe magnetic field. $\overline{\overline{D}}$ only depends upon the optical properties and upon the thicknesses of the layers: it is easily calculated, taking into account continuity conditions.

$\chi_{\eta\varepsilon}$ is derived from the equation of motion and from the boundary conditions discussed in Sec. II A. More specifically, we introduce a phenomenological damping term α (and, indeed, the probe field) in addition to the effective field. (1) is then replaced by

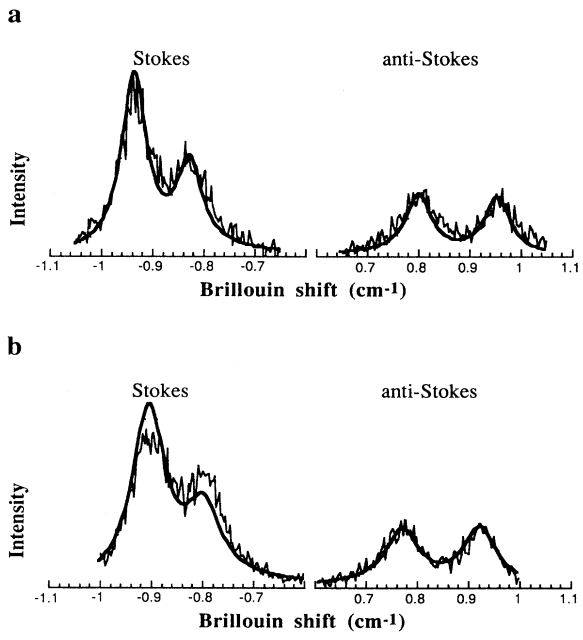

FIG. 3. Examples of calculated Stokes and anti-Stokes spectra compared to experimental results for Cu/Co/Au/Co structures. Bold lines: calculated spectra. Thin lines: experimental spectra. The two studied samples were prepared with nominal identical characteristics but the fits are provided with slightly different anisotropies [sample (a): H_a(Co/Cu)=0.41 T, H_a(Co/Au)=0.69 T; sample (b): H_a(Co/Cu)=0.51 T, H_a(Co/Au)=0.76 T]. The damping factors are identical: $\alpha=0.03$.

$$\frac{-i\omega}{\gamma}\mathbf{m}=\mathcal{M}\times\left[\mathbf{h}_p+\frac{\alpha i\omega}{M\gamma}\mathbf{m}+\mathbf{h}_d-\nabla_{\mathcal{M}}\tilde{U}^{av}+\frac{D}{M}\nabla^2\mathbf{m}+\mathbf{H}\right]. \quad (16)$$

Details of the calculation are given in the Appendix. Let us discuss and comment on some numerical results concerning the calculated intensities which appear in Figs. 3 and 4. First, the anti-Stokes spectrum significantly differs from the Stokes spectrum: this difference is particularly marked for the pseudo-Damon-Eshbach (DE) mode as previously noticed. Secondly, the spectral shape strongly depends upon the thicknesses and upon the anisotropies of the layers. In most cases, the pseudo-Damon-Eshbach mode is expected to be easily observed; in contrast, it can be difficult or practically impossible to detect the quasiuniform mode in the spectrum. Since the quasiuniform mode frequency is the most sensitive to the interlayer exchange, the geometrical arrangements of the samples have to be carefully adapted to allow the determination of this exchange. One also notices that, at least for usual values of the anisotropy fields, the situation where the anisotropy of the upper magnetic layer is significantly higher than that of the lower layer is the most favorable in order to clearly observe two distinct lines. Finally, the experimental spectra are generally well reproduced with the model used, except in some cases where the nonmagnetic layer is very thin: this will be briefly commented on in the next section.

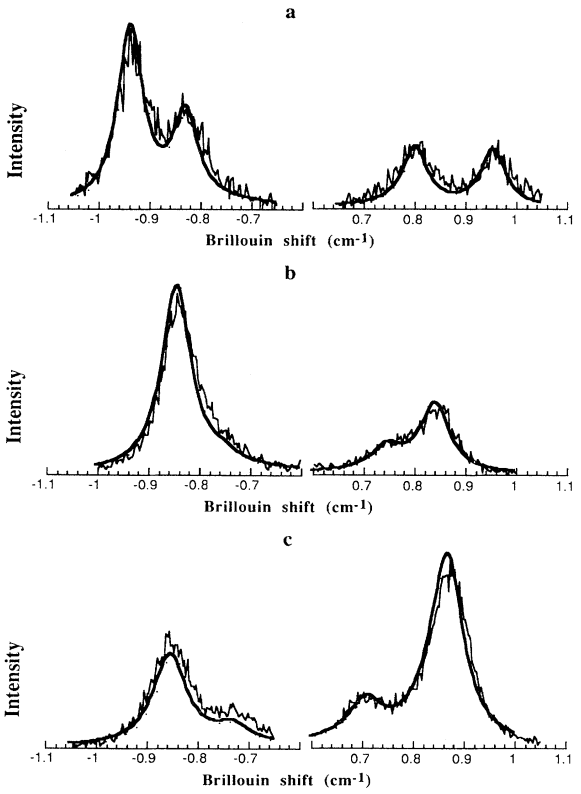

FIG. 4. Comparison of the spectra of different structures: Cu/Co/Au/Co (a), Au/Co/Au/Co (b), Au/Co/Cu/Co (c). Bold lines: calculated spectra; thin lines: experimental spectra. (a) $Si/SiO_2/Au(250)/Cu(20)/Co(75)/Au(20)/Co(75)/Au(30)$ with $H_a(Co/Cu)=0.41$ T, $H_a(Co/Au)=0.69$ T. (b) $Si/SiO_2/Au(250)/Co(75)/Au(20)/Co(75)/Au(30)$ with $H_a(Co/Au)=0.81$ T for both layers. (c) $Si/SiO_2/Au(250)/Co(50)/Cu(20)/Co(50)/Au(30)$ with $H_a(Co/Au)=1.01$ T, $H_a(Co/Cu)=0.56$ T. Applied magnetic field $H=0.4$ T for samples (a) and (b); $H=-0.4$ T for sample (c). The damping factor is $\alpha=0.03$ for all the samples.

III. RESULTS AND DISCUSSION

The following discussion is divided in two parts, dealing with the anisotropy and with the interlayer exchange, respectively. As pointed out here above, depending upon the specific information desired, the samples have to be prepared with different geometrical characteristics.

A. Anisotropies

Anisotropies were systematically investigated for samples grown on a Si substrate as a function of the thickness of the magnetic layers and of the succession of interfaces. First, in all cases, the effective anisotropy fields are nearly equal if the two magnetic layers are evaporated on identical sublayers (Cu or Au) while they markedly differ if they are evaporated on distinct sublayers (e.g., Au/Co/Cu/Co or Cu/Co/Au/Co structures instead of Cu/Co/Cu/Co or Au/Co/Au/Co). Secondly, for a magnetic layer of given thickness, the anisotropy field principally depends upon the neighboring sublayer on which it has been evaporated. Our experimental results thus suggest that the surface anisotropy energy only weakly depends upon the nature of the studied interfaces. In contrast, the nature of the neighboring sublayer monitors the volume uniaxial anisotropy energy which, as predicted, is higher for a pseudohexagonal magnetic layer (grown on Au) than for a pseudocubic one (grown on Cu).

As shown in Fig. 5, for each layer, $e\tilde{K}$ varies linearly with e, where e is the magnetic layer thickness. For a given sample with a steplike variation of e [more specifically the studied structure corresponds to Au(250)/Co(e)/Cu(20)/Co(e)/Au(30) where the numbers in parentheses specify the thicknesses in Å and e varies from 20 to 70 Å], the slope provides $K=3.1\times10^6$ erg cm^{-3} for a layer evaporated on Au and $K=3.6\times10^5$ erg cm^{-3} for a layer evaporated on Cu. The more pronounced hexagonal character expected with Co grown on Au explains this marked difference. Notice that the value 3.1×10^6 erg cm^{-3} approaches the anisotropy found in bulk hcp Co (4.5×10^6 erg cm^{-3}). Various values of k ranging from a nearly vanishing contribution to 1 erg cm^{-2} and even more can be found in the literature.[1] From the above-defined linear variation shown in Fig. 5, we derive a k value of 0.83 erg cm^{-2}, identical for both films. Previously published determinations[6,8,9] of k_{Cu} and k_{Au} concerning films grown in comparable conditions, but generally significantly thinner than those used in the present study, provide rather smaller values of $k_{Cu}(\sim0.2$ erg cm$^{-2})$ and $k_{Au}(\sim0.4$ erg cm$^{-2})$. In very

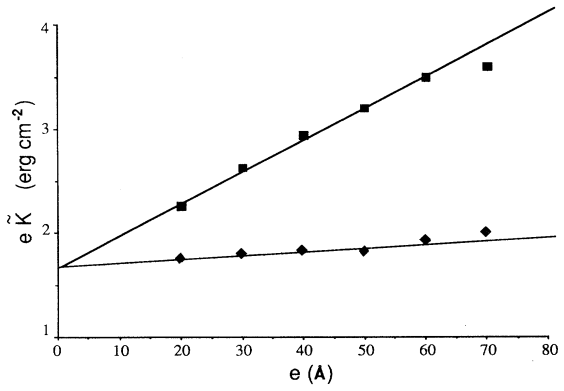

FIG. 5. Variation of $e\tilde{K}$ versus the magnetic layer thickness e for a Si/SiO_2/Au(250)/Co(e)/Cu(20)/Co(e)/Au(30) structure. ■ Experimental values for the inner layer (Au/Co). ♦ Experimental values for the outer layer (Cu/Co). Full lines: fitted linear variations assuming $4\pi M = 1.76$ T, $\gamma = 1.90 \times 10^7$ Hz Oe^{-1}. Fitted parameters: $k = 0.83$ erg cm^{-2}, $K = 3.6 \times 10^5$ erg cm^{-3} for Cu/Co, $K = 3.1 \times 10^6$ erg cm^{-3} for Au/Co.

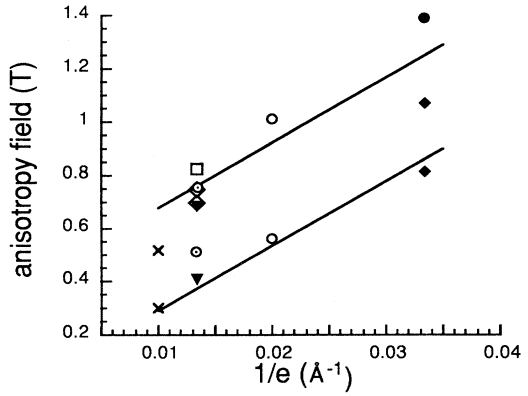

FIG. 6. Comparison of the measured anisotropy fields in various studied structures, with the expected values derived from the linear variations shown in Fig. 5. The residual discrepancies presumably derive from uncontrollable volume anisotropy variations. Notice on sample ◇ that the two magnetic layers show slightly different anisotropies. ◇, □: Si/SiO_2/Au(250)/Co(75)/Au(d)/Co(75)/Au(30), ▼, ⊙: Si/SiO_2/Au(250)/Cu(20)/Co(75)/Au(d)/Co(75)/Au(30), ×: Si/SiO_2/Au(250)/Co(100)/Cu(d)/Co(100)/Au(30), ○: Si/SiO_2/Au(250)/Co(50)/Cu(d)/Co(50)/Au(30), ♦: Si/SiO_2/Au(250)/Co(30)/Cu(d)/Co(30)/Au(30), and ●: Si/SiO_2/Au(250)/Co(30)/Au(d)/Co(30)/Au(30).

thin samples, the magnetoelastic energy does not affect the surface anisotropy and, consequently, these low values are more or less explicitly identified as purely magnetocrystalline contributions. In contrast, we think that in our rather thick samples the magnetoelastic terms are predominant or, at least, comparable to the magnetocrystalline ones in the evaluation of the surface anisotropy. Such a hypothesis agrees with the small volume anisotropy which is found in our samples, proving that the magnetoelastic contribution to the volume anisotropy is small or negligible, in contrast with the observed behavior of thinner films. We have recently obtained additional results involving rather thin (down to 10 Å) "symmetric" single magnetic layers (Cu/Co/Cu or Au/Co/Au) grown on oxidized silicon substrates: in the case of Cu/Co interfaces, we obtain a linear variation of $e\tilde{K}(e)$ with a k value lying around 0.4 erg cm^{-2}, which is closer to the 0.2 erg cm^{-2} determination mentioned above; in the case of Au/Co interfaces, $e\tilde{K}(e)$ does not obey a linear variation. Up to now a comparison with the experiments involving two magnetic layers is not straightforward. But it is clear that in the last case a surfacelike magnetoelastic contribution is present and that one observes a linear variation of $e\tilde{K}(e)$ in the 20–70 Å interval of magnetic thicknesses. The values of k and K derived from the above-described study of films containing two magnetic layers provide a reasonable estimation of the anisotropy fields of all the other samples designed for the study of the oscillatory exchange (see below), as shown in Fig. 6. Indeed, some non-negligible discrepancies remain and to give account of the observed spectra one has to find the values of the anisotropies for each sample which provide the most appropriate fit. Notice, for instance, that with a sample consisting of two magnetic layers evaporated on identical sublayers (Cu or Au) the two corresponding anisotropies can show small but not completely negligible differences.

The results concerning samples grown on a glass substrate do not markedly differ from the above determinations. We performed a systematic study for a Co layer evaporated on a Au buffer, a situation where the Co film structure is predicted to be approximately hexagonal: more precisely the sample consisted of a glass/Au(250)/Co(e)/Au(30) system with a steplike variation of the Co thickness e. The results are shown in Fig. 7. For e ranging from 40 to 90 Å, $e\tilde{K}$ varies quasilinearly with e, providing an effective value of k of about 1.26 erg cm^{-2} higher than in the case of a Si substrate. Figure 7 allows one to derive a value of K of about 7.7×10^5

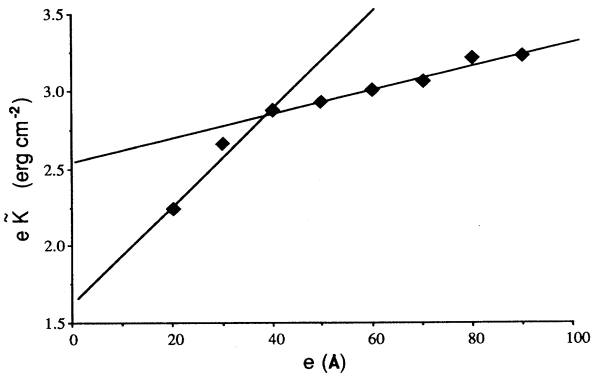

FIG. 7. Variation of $e\tilde{K}$ versus the magnetic layer thickness e for a float glass/Au(250)/Co(e)/Au(30) structure. ♦: Experimental values (assuming $4\pi M = 1.76$ T, $\gamma = 1.90 \times 10^7$ Hz G^{-1}). Full line: fitted linear variation. Fitted parameters: for low thicknesses $k = 0.81$ erg cm^{-2}, $K = 3.2 \times 10^6$ erg cm^{-3}: for high thicknesses $k = 1.26$ erg cm^{-2}, $K = 7.7 \times 10^5$ erg cm^{-3}.

erg cm^{-3}. This value is smaller than the obtained one using a Si substrate, which seems to indicate a more pronounced hexagonal character in the last case. However, the above-mentioned linear variation does not hold for the lowest studied values of e (20 and 30 Å) where the observed behavior well fits the measured one using a silicon substrate: due to the rather small number of experimental results concerning our thinner films, the last data have to be commented only speculatively. The apparent occurrence in Fig. 7 of two different slopes depending upon the Co thicknesses can be due to a change in the relaxation mechanisms related to two distinct regimes of strains in the films, as previously observed,[9] giving rise to different magnetoelastic contributions; it can also derive from the fact that the quasihexagonal structure which generates a large volume anisotropy does not persist above $e=40$ Å; such hexagonal→cubic transformations have been reported previously.[26] In any case the "effective" k determinations lie between 0.8 and 1.3 erg cm^{-2}, which is significantly higher than most of the previously published ones and undoubtedly related to magnetoelastic effects. Concerning the volume contribution, the comparison of all the experimental results strongly suggests that it varies significantly from sample to sample and, up to now, cannot be completely controlled. Consequently, the above study provides good information about the behavior of the anisotropy but does not allow a precise prediction of its value which, in each sample, has to be measured.

As mentioned above, the shapes of the Brillouin spectra strongly depend upon the anisotropy. Figures 3 and 4 show some of the fits obtained for samples with two magnetic layers: in addition to the anisotropy fields the Gilbert damping factor α [see (16)] has to be adjusted. We found $\alpha=0.03$ using Si substrates and $\alpha=0.02$ with glass substrates. α is probably strongly dependent on textural defects and on the layer roughness: using atomic force microscopy measurements we have observed that the roughness is significantly higher in samples grown on Si substrates than in samples grown on glass substrates, which could explain the differences in α.

Finally, a careful theoretical study of the intensity profiles shows that, in order to observe two well-separated distinct lines in samples containing two magnetic layers, the most favorable situation corresponds to a $\cdots$ Cu/Co/Au/Co/ $\cdots$ arrangement where the first Co is the inner magnetic layer and the second one is the upper magnetic layer. Consequently, we conclude that the oscillatory interlayer magnetic exchange is easier to observe with a Au spacer than with a Cu spacer.

To summarize, our results concerning the anisotropy show that, as a first approximation, the surface anisotropy energy density does not depend upon the investigated growing conditions while the volume anisotropy energy density is strongly sample dependent and tends to be larger for magnetic layers evaporated on a Au sublayer than for magnetic layers grown on a Cu sublayer, in connection with the less pronounced hexagonal character expected in the last case: these results agree with previous observations. The obtained value of k is comparable to the other published ones and with theoretical expectations.[1,7,20] However, the measured anisotropy suffers non-negligible individual variations from sample to sample.

B. Interlayer oscillatory exchange

The variation of the interlayer exchange versus the thickness of a Au spacer is put in evidence in our Brillouin spectra for samples grown on Si and for samples grown on glass. However, small differences have been observed. In order to derive the value of A_{12}, a precise experimental protocol has to be defined.

In the case of a Si substrate we used various samples with 2 or 4 Å steplike variations of the spacer thickness. As assumed in the preceding subsection, the best results were obtained with an inner magnetic layer evaporated on Cu. More precisely, the chosen structure was defined as Si/SiO_2/Au(250)/Cu(30)/Co(75)/Au(d)/Co(75)/Au(30). To extract the A_{12} value, we assume that the anisotropies do not depend upon the spacer thickness d and then that they can be derived from the spectra obtained with the largest values of d (e.g., 28 Å) where A_{12} is vanishingly small. The estimated uncertainty on A_{12} is ≈ 0.01 erg cm^{-2}. As shown in Fig. 8, A_{12} is clearly ferromagnetic for $d \approx 16$ Å while it is undoubtedly antiferromagnetic for $d=12$ Å. For $d \geq 12$ Å the experimental shapes of the spectra agree well with the calculated ones, as evidenced in Figs. 3 and 4. Unfortunately, for thicknesses varying from 4 to 10 Å, the observed shapes completely change and cannot be fitted using the formalism derived in Sec. II. Only one line which corresponds to the DE peak appears in the spectra (Fig. 9). This behavior is probably related to pinhole defects which provide direct exchange bridges between the two magnetic layers with, consequently, the disappearance of the quasi-uniform mode but not of the pseudo-DE one. Figure 8 suggests an oscillation with a pseudoperiod of about 10 Å, i.e., of about 4 monolayers, in agreement with recently published values derived from magneto-optical and magnetoresistive measurements.[10] The amplitude of this os-

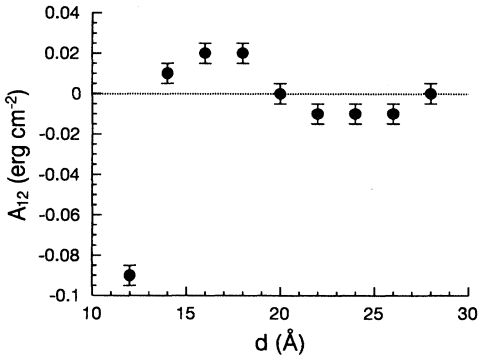

FIG. 8. Variation of the interlayer magnetic exchange versus the spacer thickness for a sample grown on an oxidized silicon substrate Si/SiO_2/Au(250)/Cu(20)/Co(75)/Au(d)/Co(75)/Au(30). Fitted anisotropy fields: H_a(Co/Cu)=0.51 T, H_a(Co/Au)=0.76 T.

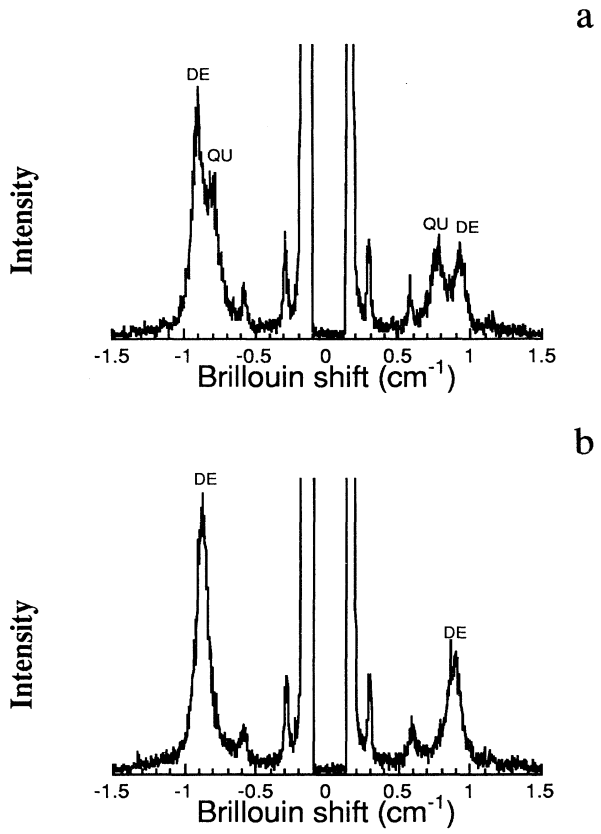

FIG. 9. Two experimental spectra for a sample grown on an oxidized silicon substrate, $Si/SiO_2/Au(250)/Cu(20)/Co(75)/Au(d)/Co(75)/Au(30)$. DE refers to the Damon-Eshbach mode. QU refers to the quasiuniform mode. Lines without index are associated with phonons: their shift does not depend upon **H**. (a) $d=14$ Å (all the lines appear on this spectrum). (b) $d=8$ Å (only the Damon-Eshbach line exists in this spectrum).

cillation exceeds by about a factor of 2 the previously published one. The oscillating behavior of A_{12} was confirmed by a Brillouin study of four different samples, including samples with magnetic layers showing nearly equal anisotropies (Au/Co/Au/Co/Au structures) where the variation of A_{12} is significantly more difficult to detect. In all cases A_{12} is found antiferromagnetic for $d=12$ Å and ferromagnetic for $d=16$ Å.

In the case of a glass substrate, we used the same protocol with a glass/Au(250)/Cu(30)/Co(75)/Au(d)/Co(75)/Au(30) sample. Here, the A_{12} variation can be followed down to $d=8$ Å; an antiferromagnetic minimum is clearly observed for $d\approx 10$ Å, as shown in Fig. 10. The better quality of the films which is confirmed by roughness measurements and by the smaller value of the Gilbert damping coefficient explains that smaller d values can provide significant results with this substrate. However, below $d=8$ Å the spectra behave as above described in samples grown on Si for small d values. The A_{12} oscillation can be fitted with the expression[15]

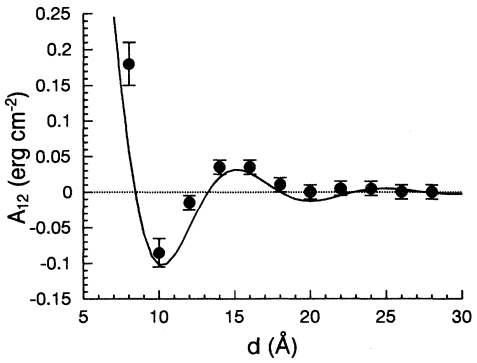

FIG. 10. Variation of the interlayer magnetic exchange versus the spacer thickness for a sample grown on a glass substrate, float glass/Au(250)/Cu(20)/Co(75)/Au(d)/Co(75)/Au(30). ●: experimental determinations [with the fitted values H_a(Co/Cu)=0.33 T, H_a(Co/Au)=0.42 T]. Full line: fit of the experimental data with expression (17) using $\mathcal{A}=4.9$ erg cm^{-2}, $d_1=9.6$ Å, $d_2=12$ Å, and $\varphi=0.78$ rad.

$$A_{12}=-\mathcal{A}\sin(2\pi d/d_1+\varphi)e^{-d/d_2}(d_0/d)^2\,, \qquad (17)$$

where d_0 is the distance between two Au atomic planes. Bruno and Chappert calculated $d_1=11.4$ Å (i.e., 4.83 monolayers) and $d_2=11.8$ Å (i.e., 5 monolayers);[15] recently, Grolier *et al.* found $d_1=10.6$ Å and $d_2=11.8$ Å from magneto-optical and magnetoresistive measurements.[10] In Fig. 10 we present a fit to our Brillouin results: it provides $d_1=9.6$ Å and $d_2=12$ Å. Due to experimental uncertainties, these values do not differ from the previous determinations and the Brillouin study confirms the existing theoretical predictions. Up to now, the $\mathcal{A}$ and φ values cannot be directly evaluated in the Bruno and Chappert model. Experimentally our determinations are significantly different from the results of Grolier *et al.*: we find $\mathcal{A}=4.9$ erg cm^{-2} and $\varphi=0.78$ rad, to compare to the Grolier *et al.* determinations $\mathcal{A}=2.7$ erg cm^{-2} and $\varphi=0.11$ rad. It is interesting to notice that, here again, as in the case of a Si substrate, we find an amplitude of oscillation larger than the previously published one.

Our experimental data concerning the Si substrate do not really allow us to fit the behavior of A_{12} with expression (17): however, it seems that the phase φ is significantly different with a Si substrate, which leads to a shift of the first ferromagnetic maximum (≈ 17 Å instead of 15 Å in the case of a glass substrate).

The oscillatory behavior of the interlayer exchange with a Cu spacer has been reported but it is strongly sample dependent and very different values have been found for its amplitude.[12] It seems admitted that, in samples evaporated in ultrahigh vacuum, pinhole defects easily appear and that they prevent observation of the oscillating exchange interaction.[21] In our Brillouin measurements we were not successful in putting this oscillation in evidence. As discussed above, the situation where the upper magnetic layer is evaporated on Cu is not favorable from the point of view of the shape of the spectra induced

by the anisotropy. From a detailed analysis of our experimental data, we can only derive an upper limit of 0.01 erg cm^{-2} for $|A_{12}|$.

To summarize, we did not observe any measurable variation of the interlayer exchange in Co/Cu/Co structures. In contrast, we confirm the existence of an oscillatory variation of the interlayer exchange versus the spacer thickness for Co/Au/Co structures: the pseudoperiodicity and the attenuation length agree, within the experimental uncertainties, with the published experimental determinations and with theoretical calculations. Finally, we have evidenced the importance of a proper choice of adjustable parameters like the thickness of the magnetic layers and the applied field, in order to get significant information about the interlayer exchange.

ACKNOWLEDGMENTS

We gratefully acknowledge M. Galtier for her contribution in preparing the studied samples. We are thankful to C. Chappert, to J. Ferré, and to J. P. Renard for fruitful discussions about the manuscript.

APPENDIX

Calculation of the Brillouin frequency shifts

Assuming that $\mathbf{m}$ is proportional to $\exp[i(Q_{\parallel}y+Q_x x-\omega t)]$, Eqs. (1)–(3) enable one to obtain the dispersion relation (A1) for a layer where $\tilde{U}^{av}=-(\tilde{K}/\mathcal{M}^2)\mathcal{M}_x^2$:

$$\begin{aligned}[H-\tilde{H}_a+D(Q_{\parallel}^2+Q_x^2)][H+D(Q_{\parallel}^2+Q_x^2)](Q_x^2+Q_{\parallel}^2)\\ -(\omega/\gamma)^2(Q_x^2+Q_{\parallel}^2)\\ +4\pi M\{Q_{\parallel}^2[H-\tilde{H}_a+D(Q_x^2+Q_{\parallel}^2)]\\ +Q_x^2[H+D(Q_{\parallel}^2+Q_x^2)]\}=0 \qquad \text{(A1)}\end{aligned}$$

with $\tilde{H}_a=2\tilde{K}/M$. Q_x^2 is a solution of a polynomial equation of degree 3; consequently, the most general expansion for $\mathbf{m}$ or $\mathbf{h}_d$ with given values of $Q_{\parallel}$ and ω is a linear combination of six different $\exp[i(Q_{\parallel}y+Q_x^j x-\omega t)]$ terms. The total number of independent coefficients describing a spin wave in each layer is reduced to six by introducing a potential ϕ such as $\mathbf{h}_d=\nabla\phi$ as deduced from (3),

$$\phi=\sum_{j=1}^{6}\Phi^j\exp[i(Q_{\parallel}y+Q_x^j x-\omega t)] .$$

The oscillating part of the magnetization

$$\mathbf{m}=\sum_{j=1}^{6}\mathbf{m}^j\exp[i(Q_{\parallel}y+Q_x^j x-\omega t)]$$

is then obtained from (1) as a function of

$$\mathbf{h}_d=\sum_{j=1}^{6}\mathbf{h}^j\exp[i(Q_{\parallel}y+Q_x^j x-\omega t)]$$

since for each allowable value Q_x^j

$$\begin{bmatrix} -i\dfrac{\omega}{\gamma} & H+D\|Q\|^2 \\ H-\tilde{H}_a+D\|Q\|^2 & i\dfrac{\omega}{\gamma}\end{bmatrix}\begin{bmatrix}m_x^j\\ m_y^j\end{bmatrix}=M\begin{bmatrix}h_y^j\\ h_x^j\end{bmatrix} \qquad \text{(A2)}$$

and $m_z^j=0$ with $\|Q\|^2=(Q_x^j)^2+Q_{\parallel}^2$, $h_y^j=iQ_{\parallel}\Phi^j$, and $h_x^j=iQ_x^j\Phi^j$.

In the case of two coupled layers, the 2×6 coefficients Φ^j are solutions of 12 linear homogeneous equations deduced from the boundary conditions. The eigenfrequencies are obtained by canceling the associated determinant.

Calculations of the Brillouin line intensities

Since $\mathbf{k}_{\parallel}^s=k_y\mathbf{e}_y$, the operator

$$\bar{\bar{L}}_x=\left[\frac{\omega^s}{c}\right]^2\varepsilon(x)-\nabla\times\nabla\times$$

can be written as

$$\bar{\bar{L}}_x=\begin{bmatrix} \left[\dfrac{\omega^s}{c}\right]^2\varepsilon-k_y^2 & -ik_y\dfrac{\partial}{\partial x} & 0 \\ -ik_y\dfrac{\partial}{\partial x} & \left[\dfrac{\omega^s}{c}\right]^2\varepsilon+\dfrac{\partial^2}{\partial x^2} & 0 \\ 0 & 0 & \left[\dfrac{\omega^s}{c}\right]^2\varepsilon+\dfrac{\partial^2}{\partial x^2}-k_y^2\end{bmatrix} . \qquad \text{(A3)}$$

Since by definition $\bar{\bar{L}}_x\bar{\bar{D}}(x,x')=\bar{\bar{I}}\delta(x-x')$ where $\bar{\bar{I}}$ is the identity operator, one finds $D_{az}=D_{za}=0$ for $a=x$ or y.

With, for instance, p-polarized light $4\pi P_z=A(E_x^i m_y-E_y^i m_x)$. From (13) and (15), it thus results for this polarization that

$$\begin{aligned}I(\mathbf{k}_{\parallel}^s,\omega^s)\propto\frac{1}{\omega}\int dx'dx''D_{zz}(x,x')D_{zz}^*(x,x'')\\ \times\{E_x^i(x')E_x^{*i}(x'')\mathrm{Im}\chi_{yy}(x'',x',\mathbf{Q}_{\parallel},\omega)+E_y^i(x')E_y^{*i}(x'')\mathrm{Im}\chi_{xx}(x'',x',\mathbf{Q}_{\parallel},\omega)\\ -E_x^i(x')E_y^{*i}(x'')\mathrm{Im}\chi_{xy}(x'',x',\mathbf{Q}_{\parallel},\omega)-E_y^i(x')E_x^{*i}(x'')\mathrm{Im}\chi_{yx}(x'',x',\mathbf{Q}_{\parallel},\omega)\} . \qquad \text{(A4)}\end{aligned}$$

(i) $D_{zz}(x,x')$ has to be known only for x' values belonging to a magnetic layer and for x outside of the sample. However, in order to determinate $D_{zz}(x,x')$, one needs to write continuity relations for D_{zz} and $(\partial/\partial x)D_{zz}$ at each interface; it is then necessary to consider values of x sweeping every domain. Notice that if x and x' do not belong to the same domain, the Dirac term is absent and that D_{zz} is a simple combination of two exponentials; when x and x' belong to the same domain the Dirac term induces an additional particular solution. Knowing the general solution for any above-mentioned (x,x') pair, the $D_{zz}(x,x')$ functions of interest can be calculated using the boundary conditions.

(ii) The exciting fields $\mathbf{E}^i$ is a linear combination of damped plane waves and is obtained in each layer versus the outside incident electric field by writing the usual boundary conditions between domains of different permittivities

(iii) In order to derive the susceptibilities required for the calculation of the scattered intensity, one introduces a probe field $\mathbf{h}_p$. From $\mathbf{h}_d=\nabla\phi$, (16) and (3) transform as

$$\frac{-i\omega}{\gamma}\mathbf{m}=\mathcal{M}\times\left[\mathbf{h}_p+\frac{\alpha i\omega}{M\gamma}\mathbf{m}+\nabla\phi-\nabla_{\mathcal{M}}\tilde{U}^{av}+\frac{D}{M}\nabla^2\mathbf{m}+\mathbf{H}\right], \tag{A5}$$

$$\nabla\cdot(4\pi\mathbf{m})+\nabla^2\phi=0 . \tag{A6}$$

The susceptibilities $\chi_{ab}(x,x',\mathbf{Q}_\parallel,\omega)$ are defined for an $f(x)\exp(i\mathbf{Q}_\parallel\mathbf{r}_\parallel-i\omega t)$ dependence of ϕ and $\mathbf{m}$. Writing

$$\phi=\Phi(x)\exp(iQ_\parallel y-i\omega t) ,$$

$$\mathbf{m}=[m_x(x)\mathbf{e}_x+m_y(x)\mathbf{e}_y]\exp(iQ_\parallel y-i\omega t) ,$$

and

$$\mathbf{h}_p=[h_x(x)\mathbf{e}_x+h_y(x)\mathbf{e}_y]\exp(iQ_\parallel y-i\omega t) ,$$

one calculates from (A5) and (A6) the appropriate susceptibilities assuming that $h_x(x)=\delta(x-x')$ and $h_y(x)=0$ or that $h_x(x)=0$ and $h_y(x)=\delta(x-x')$. More precisely, one finds the following:

(a) With $h_x(x)=\delta(x-x')$ and $h_y(x)=0$,

$$\chi_{xx}(x,x',Q_\parallel\mathbf{e}_y,\omega)=m_x(x) ,$$

$$\chi_{yx}(x,x',Q_\parallel\mathbf{e}_y,\omega)=m_y(x) .$$

(b) With $h_x(x)=0$ and $h_y(x)=\delta(x-x')$,

$$\chi_{xy}(x,x',Q_\parallel\mathbf{e}_y,\omega)=m_x(x) ,$$

$$\chi_{yy}(x,x',Q_\parallel\mathbf{e}_y,\omega)=m_y(x) .$$

It turns out that the convenient boundary conditions to be applied to the χ_{ab} functions are deduced from those for $\mathbf{m}$ and $\nabla\phi$.

Let us denote χ_{xx} as χ_{11}, χ_{yx} as χ_{21}, and Φ as χ_{31}; Eqs. (A5) and (A6) can then be written as follows:

$$\left[H'-\tilde{H}_a+D\left[Q_\parallel^2-\frac{\partial^2}{\partial x^2}\right]\right]\chi_{11}(x,x')+(i\omega/\gamma)\chi_{21}(x,x')-M\frac{\partial}{\partial x}\chi_{31}(x,x')=\delta(x-x') , \tag{A7a}$$

$$-(i\omega/\gamma)\chi_{11}(x,x')+\left[H'+D\left[Q_\parallel^2-\frac{\partial^2}{\partial x^2}\right]\right]\chi_{21}(x,x')-MiQ_\parallel\chi_{31}(x,x')=0 , \tag{A7b}$$

$$4\pi\frac{\partial}{\partial x}\chi_{11}(x,x')+4\pi iQ_\parallel\chi_{21}(x,x')+\left[\frac{\partial^2}{\partial x^2}-Q_\parallel^2\right]\chi_{31}(x,x')=0 , \tag{A8}$$

with $H'=H-\alpha i\omega/\gamma$. On the other hand, Eqs. (A7b) and (A8) are always verified if we assume

$$\chi_{11}=\left\{\left[H'+D\left[Q_\parallel^2-\frac{\partial^2}{\partial x^2}\right]\right]\left[Q_\parallel^2-\frac{\partial^2}{\partial x^2}\right]+4\pi MQ_\parallel^2\right\}\Lambda ,$$

$$\chi_{21}=\left\{4\pi MiQ_\parallel\frac{\partial}{\partial x}+(i\omega/\gamma)\left[Q_\parallel^2-\frac{\partial^2}{\partial x^2}\right]\right\}\Lambda ,$$

$$\chi_{31}=4\pi\left\{-(\omega/\gamma)Q_\parallel+\left[H'+D\left[Q_\parallel^2-\frac{\partial^2}{\partial x^2}\right]\right]\frac{\partial}{\partial x}\right\}\Lambda .$$

On the other hand, relation (A7a) leads to the equation

$$\left\{\left[H'-\tilde{H}_a+D\left[Q_\parallel^2-\frac{\partial^2}{\partial x^2}\right]\right]\left[H'+D\left[Q_\parallel^2-\frac{\partial^2}{\partial x^2}\right]\right]\left[Q_\parallel^2-\frac{\partial^2}{\partial x^2}\right]-(\omega/\gamma)^2\left[Q_\parallel^2-\frac{\partial^2}{\partial x^2}\right]+4\pi M\left\{Q_\parallel^2\left[H'-\tilde{H}_a+D\left[Q_\parallel^2-\frac{\partial^2}{\partial x^2}\right]\right]-\frac{\partial^2}{\partial x^2}\left[H'+D\left[Q_\parallel^2-\frac{\partial^2}{\partial x^2}\right]\right]\right\}\right\}\Lambda=\delta(x-x') . \tag{A9}$$

The method to find the solution is analogous to the method used for finding D_{zz}. Λ is a linear combination of exponential functions plus, when x and x' belong to the same domain, a particular solution induced by the Dirac term. Writing the boundary conditions, one finally calculates the appropriate susceptibilities [in order to write the boundary conditions related to the Maxwell equations, one has to take into account the oscillating field existing in the nonmagnetic layers which is still written as $\mathbf{h}_d=\nabla\phi$ but it now satisfies $\nabla^2\phi=0$, i.e., $(Q_\parallel^2-\partial^2/\partial x^2)\phi=0$ and is then a combination of two exponential functions].

[1]B. Heinrich and J. F. Cochran, Adv. Phys. **42**, 523 (1993).
[2]J. V. Harzer, B. Hillebrands, R. L. Stamps, G. Güntherodt, D. Weller, Ch. Lee, R. F. C. Farrow, and E. E. Marinero, J. Magn. Magn. Mater. **104**, 1863 (1992).
[3]C. M. Falco and B. N. Engel, Appl. Surf. Sci. **60**, 790 (1992).
[4]P. Krams, B. Hillebrands, G. Güntherodt, K. Spörl, and D. Weller, J. Appl. Phys. **69**, 5307 (1991).
[5]J. F. Cochran, J. M. Rudd, M. From, B. Heinrich, W. Bennett, W. Schwarzacher, and W. F. Egelhoff, Jr., Phys. Rev. B **45**, 4676 (1992).
[6]P. Beauvillain, C. Chappert, V. Grolier, R. Mégy, S. Ould-Mahfoud, J. P. Renard, and P. Veillet, J. Magn. Magn. Mater. **121**, 503 (1993).
[7]S. Ould-Mahfoud, R. Mégy, N. Bardou B. Bartenlian, P. Beauvillain, C. Chappert, J. Corno, B. Lecuyer, G. Sczigel, P. Veillet, and D. Weller, in *Magnetic Ultrathin Films: Multilayers and Surfaces/Interfaces and Characterization,* edited by B. T. Jonker, S. A. Chambers, R. F. C. Farrow, C. Chappert, R. Clarke, W. J. M. de Jonge, T. Egami, P. Grünberg, K. M. Krishnan, E. E. Marinero, C. Rau, and S. Tsunashima, MRS Symposia Proceedings No. 313 (Materials Research Society, Pittsburgh, 1993), p. 251.
[8]J. Kohlhepp, H. J. Elmers, and U. Gradmann, J. Magn. Magn. Mater. **121**, 487 (1993).
[9]B. Hillebrands, P. Krams, J. Faβbender, C. Mathieu, and G. Güntherodt, Acta Phys. Pol. A **85**, 179 (1994).
[10]V. Grolier, D. Renard, B. Bartenlian, P. Beauvillain, C. Chappert, C. Dupas, J. Ferré, M. Galtier, E. Kolb, M. Mulloy, J. P. Renard, and P. Veillet, Phys. Rev. Lett. **71**, 3023 (1993).
[11]J. J. de Vries, P. J. H. Bloemen, M. T. Johnson, J. aan de Stegge, A. Reinders, and W. J. M. de Jonge, J. Magn. Magn. Mater. **129**, L129 (1994).
[12]M. T. Johnson, R. Coehoorn, J. J. de Vries, N. W. E. McGee, J. aan de Stegge, and P. J. H. Bloemen, Phys. Rev. Lett. **69**, 969 (1992).
[13]J. Faβbender, F. Nörtemann, R. L. Stamps, R. E. Camley, B. Hillebrands, G. Güntherodt, and S. S. P. Parkin, Phys. Rev. B **46**, 5810 (1992).
[14]W. F. Egelhoff, Jr., and M. T. Kief, Phys. Rev. B **45**, 7795 (1992).
[15]P. Bruno and C. Chappert, Phys. Rev. B **46**, 261 (1992).
[16]J. F. Cochran, J. M Rudd, W. B. Muir, B. Heinrich, and Z. Celinski, Phys. Rev. B **42**, 508 (1990).
[17]P. Grünberg, J. Barnás, F. Sauerenbach, J. A. Fuβ, A. Wolf, and M. Vohl, J. Magn. Magn. Mater. **93**, 58 (1991).
[18]B. Heinrich, Z. Celinski, J. F. Cochran, W. B. Muir, J. Rudd, Q. M. Zhong, A. S. Arrott, K. Myrtle, and J. Kirschner, Phys. Rev. Lett. **64**, 673 (1990).
[19]T. Kingetsu and K. Sakai, Phys. Rev. B **48**, 4140 (1993).
[20]C. Chappert and P. Bruno, J. Appl. Phys. **64**, 5736 (1988).
[21]S. S. P. Parkin, R. F. Marks, R. F. C. Farrow, G. R. Harp, Q. H. Lam, and R. J. Savoy, Phys. Rev. B **46**, 9262 (1992).
[22]P. Grünberg, S. Demokritov, A. Fuβ, and J. A. Wolf, J. Appl. Phys. **69**, 4789 (1991).
[23]S. P. Vernon, S. M. Lindsay, and M. B. Stearns, Phys. Rev. B **29**, 4439 (1984).
[24]M. Vohl, J. A. Wolf, P. Grünberg, K. Spörl, D. Weller, and B. Zeper, J. Magn. Magn. Mater. **93**, 403 (1991).
[25]B. Hillebrands, J. V. Harzer, R. L. Stamps, G. Güntherodt, C. D. England, and C. M. Falco, J. Magn. Magn. Mater. **93**, 211 (1991).
[26]K. Le Dang (private communication).
[27]M. Vohl, J. Barnás and P. Grünberg, Phys. Rev. B **39**, 12 003 (1989).
[28]B. Hillebrands, Phys. Rev. B **41**, 530 (1990).
[29]P. Grünberg, *Light Scattering from Spin-Waves in Thin Films and Layered Magnetic Structures,* Light Scattering in Solids Vol. V, edited by M. Cardona and G. Güntherodt (Springer-Verlag, Berlin, 1989), p. 303.
[30]R. E. Camley and D. L. Mills, Phys. Rev. B **18**, 4821 (1978).

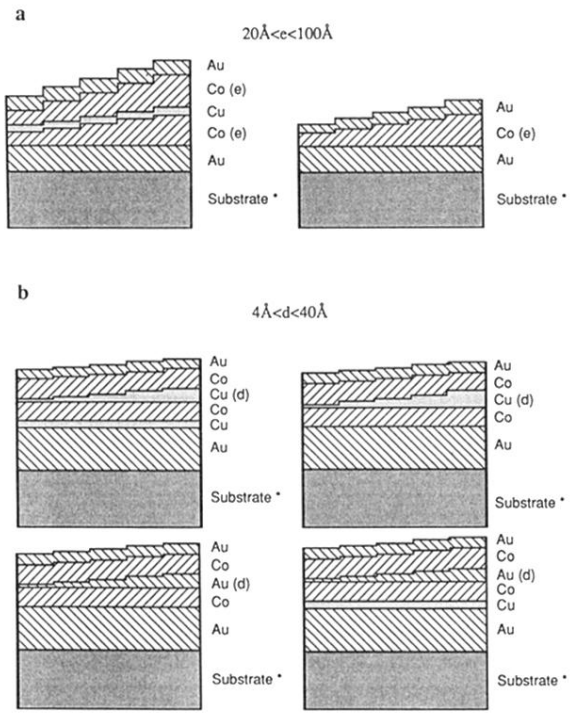

FIG. 1. Typical studied structures. (a) Samples with variable thickness of the magnetic layer(s) (steplike variation with 10 Å steps: $20 < e < 100$ Å) designed in order to study the anisotropy. (b) Samples with variable thickness of the nonmagnetic spacer (steplike variation with 2 Å steps: $4 < d < 40$Å) designed in order to study the interlayer exchange. The substrate is oxidized Si [Si/SiO_2 (2000 Å)] or float glass.